Article

Journal of the Brazilian Chemical Society

https://dx.doi.org/10.21577/0103-5053.20230095

J. Braz. Chem. Soc. **2024**, *35*, 1, e-20230095, 1-12

Revisiting the Synthesis of Gibbsite, a Precursor for Li/Al LDH Synthesis and Its Use as a Support for Porphyrin Immobilization

Gabriela Bosa,[a] Caroline G. Silva,[a] Bianca R. Brito,[a] Carolina M. Terzi,[a,b] Fernando Wypych[b] and Shirley Nakagaki[*,a]*

[a]*Laboratório de Bioinorgânica e Catálise, Departamento de Química, Centro Politécnico, Universidade Federal do Paraná (UFPR), 81531-980 Curitiba-PR, Brazil*

[b]*Laboratório de Química de Materiais Avançados, Departamento de Química, Centro Politécnico, Universidade Federal do Paraná (UFPR), 81531-980 Curitiba-PR, Brazil*

In this work, some of the synthesis methods already reported for aluminum(III) hydroxide polymorphs with layered structure like gibbsite are revisited. Gibbsite was synthesized with high purity and yield by a simple route developed from modifications of a heating method proposed in the literature, making it possible to prepare gibbsite in regular glassware, avoiding the use of hydrothermal reactor and oven, as described in the literature. The proposed synthesis was conducted with a heating system under reflux conditions in a glass heating flask, using an oil bath, without the need for more sophisticated equipment. This is an accessible alternative method for crystalline gibbsite synthesis, with yield (76 wt.%). The obtained gibbsite was used as a precursor for the synthesis of a lithium/aluminum layered double hydroxide (LDH) from the intercalation method of $Al(OH)_3$ in aqueous solution of lithium chloride. Gibbsite and the obtained LDH Li/Al were used for the immobilization of an anionic porphyrin with a loading on the order of 10^{-5} mol g^{-1} of solid, thus being alternative solid supports for catalytic species such as porphyrins.

Keywords: porphyrin, layered double hydroxide, gibbsite, intercalation, immobilization

Introduction

Layered compounds are a class of materials with stacking of two-dimensional inorganic units (layers), which can be electronically neutral or charged depending on their chemical composition and bonding. These layers are bound together by van der Waals forces or by electrostatic interactions with the molecules or ions possibly present in the interlayer space.[1,2] The minerals brucite ($Mg(OH)_2$) and gibbsite ($Al(OH)_3$) have structures that are commonly used to describe and understand the structure of various synthetic layered compounds.

In brucite structure, the layers are obtained by sharing edges of octahedra with Mg^{2+} cations at the center, coordinated to six hydroxide anions, resulting in a trioctahedral structure. Since each Mg^{2+} ion is coordinated by six hydroxide anions, each bond involves a 2/6 = 1/3 positive charge, and since each hydroxide anion is bound to three Mg^{2+} ions, each bond involves a negative charge of 1/3. Thus, the charges cancel each other out and the layers are electronically neutral.[1]

In gibbsite, each Al^{3+} cation is coordinated to six hydroxide anions, with an octahedral geometry, similar to Mg^{2+} in brucite, but aluminum cations have a 3+ charge, so each bond involves a 3/6 = 1/2 positive charge. To keep the electroneutrality of the layer, each hydroxide anion is bound to only two Al^{3+} cations, resulting in a negative charge of 1/2 on each bond. Thus, in gibbsite one-third of the octahedral centers are unoccupied, forming a structure called dioctahedral.[3]

The structure of a class of layered compounds called layered double hydroxides (LDHs) is similar to the structure of brucite. To understand the structure of LDHs, one can imagine that part of the Mg^{2+} cations in brucite are replaced isomorphically by trivalent cations (e.g., Al^{3+} cations) providing the layer with a positive residual charge. The presence of anions in the interlayer space of this Mg/Al LDH is then necessary to balance this residual charge, resulting in a material capable of performing anion exchange reactions.

The general molecular formula of a traditional LDH can be represented as $[M^{2+}_{1-x}M^{3+}_{x}(OH)_2]^{x+}(A^{m-})_{x/m}\cdot nH_2O$, where

*e-mail: shirleyn@ufpr.br
Editor handled this article: Izaura C. N. Diógenes (Associate)

M^{2+} stands for divalent metal ions (such as Mg^{2+}, Ni^{2+}, Fe^{2+}, etc.) and M^{3+} stands for trivalent cations such as Cr^{3+}, Al^{3+}, among other ions and A^{m-} denotes the interlayer anions.[2]

Besides the composition and organization of the layers in space, the positive and negative charges exhibited by LDH solids allow the manipulation and creation of different properties in these materials, making them very versatile in terms of applications.

The ability of LDHs to selectively exchange anions is an indication that these materials can be interesting supports for immobilization and intercalation of different species for different purposes, such as catalysis to support anionic metalloporphyrins (MP).[4,5] Solids formed by immobilization or even intercalation of MP into LDHs have already been reported in the literature, along with good results of heterogeneous catalysis involving these materials.[6-8]

An example of an unusual LDH, since it does not typically involve divalent and trivalent cations, is the solid formed from lithium salts and one of the polymorphs of aluminum hydroxide, commonly gibbsite (γ-$Al(OH)_3$). When this solid reacts with an excess of lithium salts, compounds of the type $[Li(Al(OH)_3)_2]A{\cdot}H_2O$ can be formed (A = interlayer anion, e.g., Cl^-, Br^-, NO_3^-).[9] There are also other methods to synthesize this aluminum rich LDH, such as hydrothermal or mechanochemical reactions that start from other polymorph of aluminum hydroxide to react with lithium salts or even lithium hydroxide,[9-17] the co-precipitation of lithium and aluminum salts with a base,[18-27] the homogeneous precipitation with urea,[18,27-30] the reaction of a metallic Li-Al alloys with water, and the reaction of metallic aluminum with a LiOH solution,[31,32] are among many examples.

In these materials, the presence of lithium cations in 1/3 of the octahedral positions of the layers (previously unoccupied in gibbsite, for example) and the intercalated anions in the interlayer space allow obtaining Li/Al LDH.[9,10] However, not all the mentioned methods lead to LDHs of the same polytype, because polytypes are variations resulting from different ways the layers are stacked along the basal direction, being the layers from the same composition and structure.[18]

Zhitova *et al*.[33] reviewed the crystallographic properties of lithium and aluminum layered hydroxides and identified this material as a mineral called dritsite, with ideal formula $Li_2Al_4(OH)_{12}Cl_2{\cdot}3H_2O$. This mineral is part of the group of LDHs based on precursors with layers having dioctahedral structure, such as gibbsite (γ-$Al(OH)_3$), and presents a hexagonal (2H) polytype. Furthermore, X-ray diffractometry analysis performed by the authors with the mineral led to results similar to those obtained for the LDH with formula $[Li(Al(OH)_3)_2]Cl{\cdot}H_2O$ or $[LiAl_2(OH)_6]Cl{\cdot}H_2O$, synthesized by O'Hare and co-workers.[9]

The most common hydroxylated aluminum solids are aluminum hydroxide ($Al(OH)_3$) and aluminum oxyhydroxide (AlOOH), the latter being commonly found in the form of the mineral bohemite,[34] while $Al(OH)_3$ occurs in the form of four polymorphs: gibbsite, bayerite, nordstrandite and doyleite.[35,36]

The preparation of aluminum hydroxides, like gibbsite, with different morphological, crystallinity and particle size, is of great interest nowadays since this class of compounds has many applications, including as an adsorbent of different metals/metallic ions,[37-39] dyes such as methyl orange and eriochrome black T in aqueous solutions;[40,41] as a catalyst support or precursor of catalyst synthesis such as in the synthesis of alumina[11,42-47] and zeolites.[48,49] It is also used as an adjuvant in the preparation of various types of vaccines, especially those based on inactivated microorganisms and even some vaccines developed against severe acute respiratory syndrome coronavirus 2 (SARS-CoV-2), the agent that causes coronavirus disease 2019 (COVID-19);[50-57] and as antacid drugs;[58] its structure is also used to describe or even synthesize different kinds of layered materials, such as clay minerals[59,60] and LDH,[9,15] and the study of its natural occurrence is used to explain the formation, weathering and adsorption processes in soils,[61,62] among other applications.

Many of these applications are intrinsically related to solid properties, such as particle size, crystallinity, and morphology.[18,25,42,44,56,63]

According to the literature,[64-68] depending on the aluminum hydroxide preparation route, the produced material has different characteristics. For example, large gibbsite particles (of the order of tens of micrometers) are obtained by the industrial preparation method involving hydrothermal digestion of bauxite ore, resulting in a supersaturated solution containing sodium and aluminum ions that subsequently lead to crystallization of the desired solid in the presence of a seed, the so-called Bayer process.[69,70]

Recently, Chang *et al.*[36] prepared gibbsite nanoplates by a sol-gel method, using aluminum *tert*-butoxide under different pH conditions and obtained a solid with a beautiful star-shaped morphology.

In this work, we report the preparation of gibbsite with high yields by a simple route that does not involve hydrothermal treatment or the use of equipment (autoclave) or reactors and other glassware that are resistant to pressure and varying pH conditions, as commonly used by the authors who have described the preparation of this solid. Then, this solid was used as a source for the preparation of a Li/Al LDH. Gibbsite and Li/Al LDH were also successfully employed in the immobilization of a tetraanionic porphyrin, demonstrating their potential as

support for interesting species, such as macrocyclic ligands for different applications.

Experimental

Characterization and apparatus

For X-ray diffraction measurements, the powdered samples were deposited on glass sample holders. The measurements were obtained in the reflection mode using a Shimadzu XRD-6000 diffractometer (Kyoto, Japan) operating at 40 kV and 30 mA, using Cu Kα radiation (λ = 1.5418 Å) and a dwell time of 2° min^{-1}, and the data were collected between 3 and 70° (in 2θ).

Fourier transform infrared (FTIR) spectra were recorded with a Bruker VERTEX 70 (Billerica, Massachusetts) spectrophotometer in the 400-4000 cm^{-1} range, using KBr pellets. KBr was crushed with a small amount of the solid samples, and the spectra were recorded with an accumulation of 32 scans.

UV-Vis spectra were recorded in the 200-800 nm range with a Varian Cary 100 spectrophotometer (Melbourne, Australia). Qualitative spectra of the solid samples were also recorded by dispersion in mineral oil or methanol.

Scanning electron microscopic images (SEM) were obtained with a Tescan VEGA3LMU apparatus (Brno, Czech Republic), using tension of 10 kV. The samples were deposited on aluminum stubs and gold sputtered to obtain the SEM images.

Transmission electron microscopic (TEM) images were obtained with a JEOL-JEM 1200 microscope operating at 120 kV. The selected area electron diffraction (SAED) patterns were obtained with the same equipment. The samples were prepared by dispersion in water at room temperature and a diluted dispersion drop was deposited on a carbon film supported by a 3 mm copper grid.

Materials

All chemicals used in this study were purchased from Sigma-Aldrich/Merck (Darmstadt, Germany), Vetec (Duque de Caxias, Brazil), J. T. Baker (Phillipsburg, USA), Nuclear or Biotec (São Paulo, SP, Brazil) and were of analytical grade.

Gibbsite ($Al(OH)_3$) synthesis

The solid named Gib-1 was prepared following a modification of the procedure reported by Sohn and co-workers.[34] A condenser, a burette and a rubber septum were attached to a 500 mL three-neck round-bottom flask. To the flask was added 100 mL of an $AlCl_3 \cdot 6H_2O$ aqueous solution (0.1 mol L^{-1}) that was kept under stirring at 50 °C in an oil bath for one hour. After this time, still under stirring and heating, 128 mL of an aqueous solution of NaOH (0.3 mol L^{-1}) was slowly added dropwise (flow rate of 10 drops min^{-1}). During the addition of the base, the formation of dispersed white flakes was observed. After the base addition, the dispersion was left under reflux and stirring for 5 days. After cooling to room temperature, the obtained dispersion was mixed with 200 mL of saturated NaCl solution and vacuum filtered through a 0.45 μm pore diameter nylon membrane. The solid obtained was washed with ultrapure water until the supernatant was free of NaCl. The solid obtained was dispersed in 75 mL of water and denominated Gib-1 (yield 68.26%).

In addition, six other attempts were made to prepare gibbsite based on modifications of the method initially proposed by Shen *et al.*[64] The general procedure adopted for the synthesis of the solids named Gib-2 to Gib-7 is described below. Table 1 presents a summary of the modifications made to the general procedure for the preparation of each solid. For the general preparation of the solids named Gib-2 to Gib-7, 5.0 or 10 g of $Al(NO_3)_3 \cdot 9H_2O$ were completely dissolved in a volume of distilled water at room temperature. The pH of the salt solution (initially close to 3.1) was adjusted to 5.0 by adding dropwise an aqueous solution of 10% (m/m) NH_3 under slow and careful stirring, with the aid of a pH-meter. After continuous stirring for 10 min, a white gel-like dispersion was obtained and transferred to a round-bottomed flask immersed in a heated oil bath, connected to a reflux condenser and over a magnetic stirring system. In this step, the entire gel-like dispersion was transferred to the flask, except in the synthesis of Gib-3, in which only 33 mL of the dispersion obtained was used. The dispersion was heated and kept at 100 °C for different periods (in days) and the final solid obtained was separated by centrifugation, washed twice with distilled water, and dried in an oven at approximately 100 °C overnight. In the case of Gib-2 synthesis, after continuous stirring of the added reagents described above for 10 min, the obtained white gel-like dispersion was transferred to a poly(tetrafluoroethylene) capsule (150 mL capacity) and placed in a stainless-steel reactor vessel for hydrothermal heating in an oven at a temperature of 100 °C. The rest of the procedure was performed as described for Gib-3 to Gib-7.

Lithium aluminum LDH (LiAl) synthesis

First attempt to synthesize Li/Al LDH: based on O'Hare and co-workers[9]

All the materials synthesized to obtain lithium-aluminum LDH were named LiAl. Two attempts were made to synthesize

Table 1. Details of the experimental conditions involved in the preparation of the Gib-2 to Gib-7 solids

Solid	Al^{3+} salt[a] / g	H_2O / mL	Heating time / day	Vessel and heating equipment	Gib solid mass / g	Yield / wt.%
Gib-2	5.00	100	10	hydrothermal reactor, oven	0.5054	29
Gib-3	5.00	100	10	heating flask, oil bath	0.2904	84
Gib-4	10.00	200	10	heating flask, oil bath	1.5197	73
Gib-5	10.00	200	11	heating flask, oil bath	1.5478	74
Gib-6	10.00	200	12 + 8 h	heating flask, oil bath	1.4275	69
Gib-7	10.00	200	14	heating flask, oil bath	1.5901	76

[a]$Al(NO_3)_3{\cdot}9H_2O$.

the material $[LiAl_2(OH)_6]Cl$ according to adaptations of the method described by O'Hare and co-workers,[9] using the solids Gib-6 and Gib-7 as matrixes. These syntheses are described as follows. For LiAl-1, 0.3012 g of Gib-6 and 0.6585 g of LiCl were dispersed in 25 mL of water (Li/Al molar ratio ca. 4:1) in a 50 mL heating flask, which was connected to a reflux condenser and heated under stirring in an oil bath at 90 °C for 6 h. The solid obtained was washed five times with 15 mL of distilled water and dried in an oven at 90 °C for 2 h, yielding the material named LiAl-1 (mass 0.3022 g, yield 62%). For LiAl-2, the synthesis was similar to LiAl-1, but used 0.3030 g of Gib-7 and 0.6594 g of LiCl as precursors. The resulting solid was named LiAl-2 (mass 0.2844 g, yield 58%).

Second attempt to synthesize Li/Al LDH: using a supersaturated solution

For the synthesis of LiAl-3, in a flask, 0.0491 g of previously prepared Gib-3 and 2.5 mL of LiCl solution heated to 90 °C were added. This solution was prepared so that it was unsaturated at 90 °C and supersaturated at room temperature. The flask was kept at room temperature and after four days the solid obtained was washed thoroughly with distilled water until the supernatant no longer showed traces of chloride (tested by visible precipitation of AgCl when 2 drops of 0.1 mol L^{-1} $AgNO_3$ solution were added). The obtained solid was dried in an oven at 100 °C for about 12 h. The solid obtained was named LiAl-3 (0.0342 g, yield 48%) and characterized by powder X-ray diffraction (PXRD).

Third attempt to synthesize Li/Al LDH: based on Hou and Kirkpatrick[15]

The Li/Al LDH was synthesized by modifications to the method described by Hou and Kirkpatrick.[15] For LiAl-4, the solid Gib-7 was previously dried in an oven at 60-70 °C for 4 h, and then stored in a desiccator until reaching room temperature. In a two-neck flask, the solid Gib-7 (0.9007 g) and an aqueous LiCl solution/dispersion (1.5156 g of the salt added to 2.5 mL of previously boiled distilled, water) were added. The system was closed and placed under magnetic stirring and heating in a silicon bath at 90 °C for 14 h. After cooling to room temperature, the white paste obtained was washed for three cycles with 15 mL of previously boiled distilled water, using an ultrasound bath, in order to remove the excess of unreacted LiCl. The white solid was obtained by centrifugation, dried at room temperature for 7 days and named LiAl-4 (1.0863 g, yield 86.9%).

Anionic porphyrin immobilization on gibbsite (Gib-7) and Li/Al LDH

For Gib-7-Por or LiAl-4-Por, 25 mL of an aqueous solution of the meso-tetrakis(4-sulfonatophenyl)porphyrin with sodium counter-ions, $Na_4[H_2(TSPP)]$, was prepared (porphyrin mass: 186 mg for Gib-7-Por and 180 mg for LiAl-4-Por) and mixed with the solid support chosen (0.1073 g of the LiAl-4 or 0.1073 g of the Gib-7) in an Erlenmeyer flask. The dispersion obtained was covered and kept under magnetic stirring at room temperature for 5 h. Then, the dispersion was centrifuged, the solid was washed with distilled water three times until colorless solution is obtained and all supernatants were collected and combined to form a solution of known volume (100 mL), which was analyzed by electronic spectroscopy in the UV-Visible region (UV-Vis) to determine the loading of porphyrin (mol) in the solid (mass *per* g). The solids obtained were dried at room temperature and named Gib-7-Por and LiAl-4-Por. $\varepsilon(Na_4[H_2(TSPP)]$, water, λ / nm 412) = 284146 L cm^{-1} mol^{-1}. Immobilization percentage (wt.%): Gib-7-Por = 98.9%; LiAl-4-Por = 99.1%. Loading: Gib-7-Por = 1.3836×10^{-5} mol g^{-1}; LiAl-4-Por = 1.3419×10^{-5} mol g^{-1}.

Results and Discussion

Gibbsite ($Al(OH)_3$) synthesis

An attempt was initially made to synthesize gibbsite based on the method reported by Sohn and co-workers.[34]

By this method, the authors studied the synthesis of gibbsite and boehmite by a method similar to the one for the clay mineral imogolite, with synthesis based on the reflux of a mixture of aluminum(III) chloride and sodium hydroxide in an aqueous medium for 5 days. According to the authors, the temperature setting determines whether gibbsite or boehmite is obtained: gibbsite is obtained by synthesis at 50 °C, while boehmite is obtained by synthesis at 98 °C.

The synthesis performed in this work was slightly modified regarding the concentration of the reagents proposed by Sohn and co-workers;[34] however the temperature of 50 °C was maintained with the objective of obtaining gibbsite.

The white solid obtained and named Gib-1 was analyzed by PXRD (Figure 1). The X-ray diffraction pattern exhibited a profile similar to the pattern of ICSD 200413, which refers to bayerite, a polymorph of aluminum hydroxide (Figure 1). In addition, the formation of an amorphous halo was observed in the Gib-1 X-ray diffraction pattern, suggesting insufficient aging for the material to reach crystallinity. The method of Shen *et al.*[64] for example, which also starts from aluminum salt in an aqueous solution to obtain gibbsite, involves heating for 10 days, even though X-ray diffraction pattern containing diffraction peaks referring to gibbsite were already present on the fifth day. According to the authors, more time is needed to obtain a more crystalline $Al(OH)_3$. Moreover, there are other reports in the literature of similar syntheses in which a more basic pH favors the formation of bayerite and boehmite, while neutral or acid pH favors the synthesis of gibbsite.[64-68] The pH measurements of the reaction media, after combining the reagents in the synthesis of Gib-1, indicated values close to 10, suggesting that the basic media favored obtaining bayerite and/or boehmite under these conditions.

The crystallization of $Al(OH)_3$ was reported to be dependent on reaction temperature.[64] At temperature below 150 °C, gibbsite with various morphologies was obtained whereas a higher temperature yielded boehmite (AlOOH).[71] For this reason, we made more attempts to prepare gibbsite at a temperature in the ideal range. For the preparation of Gib-2 to Gib-7, the temperature was kept around 100 °C.

Shen *et al.*[64] also reported that the crystal growth is greatly dependent on the pH value in the crystallization medium. As indicated, under pH = 10, boehmite with a small impurity of bayerite was obtained and under neutral condition (pH = 7.0), an amorphous gel was obtained. Because of this, the pH of 5.0 was chosen to prepare the solids Gib-2 to Gib-7.

Except for Gib-1 (Figure 1c), which corresponds to bayerite, the X-ray diffraction pattern of all other Gib solids

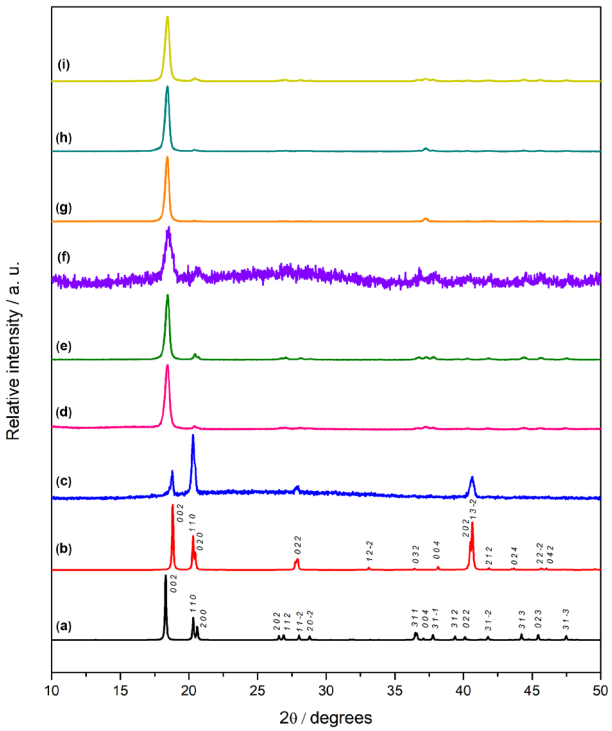

Figure 1. PXRD diffraction patterns for standards available in the literature for (a) gibbsite (ICSD 36233), (b) bayerite (ICSD 200413) and for the synthesized materials (c) Gib-1, (d) Gib-2, (e) Gib-3, (f) Gib-4, (g) Gib-5, (h) Gib-6 and (i) Gib-7.

(Figures 1d to 1i) is in good agreement with reference data for gibbsite.[72] An intense diffraction peak at the 2θ angle of 18.3° is assigned to (002) diffraction plane. The crystal structure of gibbsite is classified in a monoclinic space group (P21/n) with a = 8.684 Å, b = 5.078 Å, c = 9.736 Å and β = 94.54°.

The prepared Gib solids were analyzed by SEM (Figure 2) and TEM (Figure 3) and the images showed uniform monodisperse pseudohexagonal plates. The hydrothermally synthetic gibbsite plates had an estimated thickness of about 50 nm and a width in the range of 0.50-0.60 μm, similar to the size reported by Shen *et al.*[64] who prepared gibbsite under hydrothermal condition for 10 days, at pH 5.0 with 0.6-0.8 μm.

The SEM (Figure 2) and TEM images (Figure 3) obtained for Gib-3 indicate pseudohexagonal platelet-like particles, which are typical of gibbsite.[64] Although this synthesis had large yield (84 wt.%), it was not reproducible and produced an insufficient amount of solid to proceed with further synthesis.[64]

To obtain a greater mass of the Gib-3 material, it was decided to perform a similar synthesis, but with twice as much chemicals to synthesize the Gib-4 and Gib-6 materials. In the case of Gib-4, the material obtained exhibited a different appearance, agglomerated. After 10 days of heating, for Gib-6 synthesis, an aliquot of the

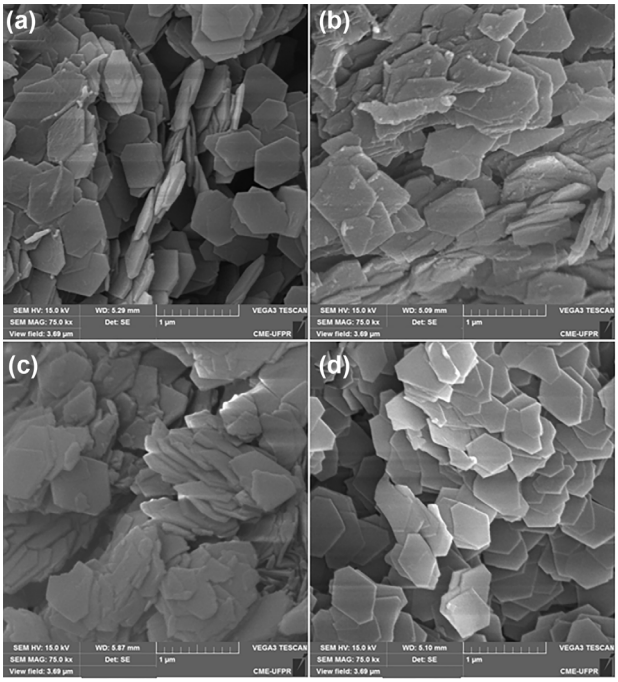

Figure 2. SEM images of materials (a) Gib-3, (b) Gib-5, (c) Gib-6 and (d) Gib-7.

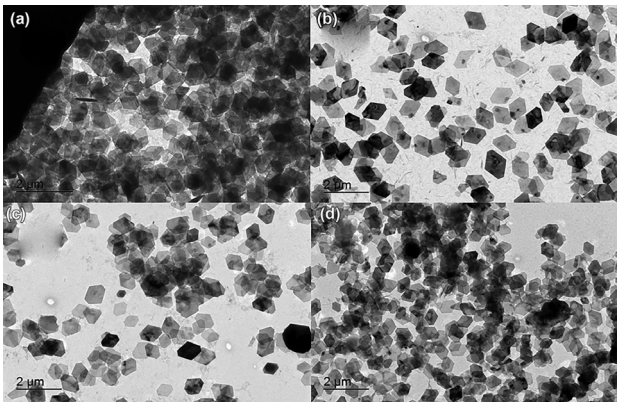

Figure 3. TEM images of materials (a) Gib-3, (b) Gib-5, (c) Gib-6 and (d) Gib-7.

reaction mixture was collected and dried for analysis by PXRD. However, it had a flaky appearance, similar to Gib-4, and could not be prepared for characterization by this technique.

Aiming to verify whether longer heating would lead to the formation of the desired material, the reaction mixture was heated for more hours, which yielded the white solid Gib-6. The X-ray diffraction pattern of this solid (Figure 1h) showed a similar profile to gibbsite. The SEM images of this material indicated particles with pseudohexagonal morphology, but highly distributed in sizes (Figure 2c).

To evaluate the effect of the heating time, syntheses similar to that for Gib-6 were performed with 11 and 14 days of heating, leading to the white solids Gib-5 and Gib-7, respectively. When comparing the X-ray diffraction patterns of these materials (Figure 1), we noticed that the solid Gib-7 presented diffraction peaks at 2θ angles around 18°, with profile and intensity more similar to the X-ray diffraction pattern of gibbsite than the solid Gib-5. The SEM images obtained for both materials (Figures 2b and 2d) indicated that the particles with pseudohexagonal morphology of Gib-7 (Figure 2d) were more defined and uniform than those of the other materials.

By comparing the mass yields of the Gib-5, Gib-6 and Gib-7 materials, we concluded that the longer the heating time, the higher the synthesis yield was (Table 1). The best Gib material obtained in sufficient quantity to proceed with the synthesis of Li/Al LDH was Gib-7.

Synthesis of lithium aluminum LDH (LiAl)

There are different strategies for obtaining one of the lithium-aluminum LDH forms, which mainly include coprecipitation processes, homogeneous precipitation with urea, hydrothermal or mechano-chemical treatments, or heating of aluminum hydroxide in solution/mixed with lithium ions under reflux.[18] The synthesis method investigated in this work was based on the reaction of gibbsite with a lithium chloride solution under reflux. Since the conditions used should not promote high dissolution of $Al(OH)_3$, the reaction should occur by intercalation of Li^+ cations in the unoccupied octahedral sites of the existing di-octahedral gibbsite layers, with corresponding intercalation of water and chloride anions to maintain the layers electroneutrality.[12] It has been reported that this synthesis method and the use of gibbsite in the reaction favors obtaining the 2H polytype of Li/Al LDH.[18,55]

Attempts to synthesize the layered solid $[LiAl_2(OH)_6]Cl{\cdot}zH_2O$ based on the method described by O'Hare and coworkers[9] were conducted using the solids Gib-6 and Gib-7. These syntheses led to the materials LiAl-1 and LiAl-2, and the absence of LDH peaks in their X-ray diffraction patterns suggests there was no formation of a layered LDH-like compound (Figure 4). The comparison was made with those of the Li/Al LDH solids containing chloride ions deposited in the Cambridge Structural Database under the identifiers ICSD 83509 and ICSD 83512 by O'Hare and coworkers.[9]

One of the possible explanations for our experimental failure in the preparation of LDH according to the method proposed by O'Hare and coworkers[9] may be related to the use of inadequate concentrations of the reagents, since few details regarding the concentration were presented by those authors.[9] The need for the gibbsite reagent to be in the presence of a solution with a high concentration of LiCl for Li/Al LDH to be formed was experimentally observed

by Hou and Kirkpatrick,[15] and the opposite has also been reported in the literature, such that excessive deintercalation of Li/Al LDH by prolonged water exposure can regenerate $Al(OH)_3$.[73,74] Since none of the gibbsite materials (Gib-6 and Gib-7) used led to Li/Al LDH, it was possible to assume that the synthesis conditions used were inadequate regarding the concentration (but not the composition) of the reagents, which prompted us to search for other methods to obtain the desired LDH.

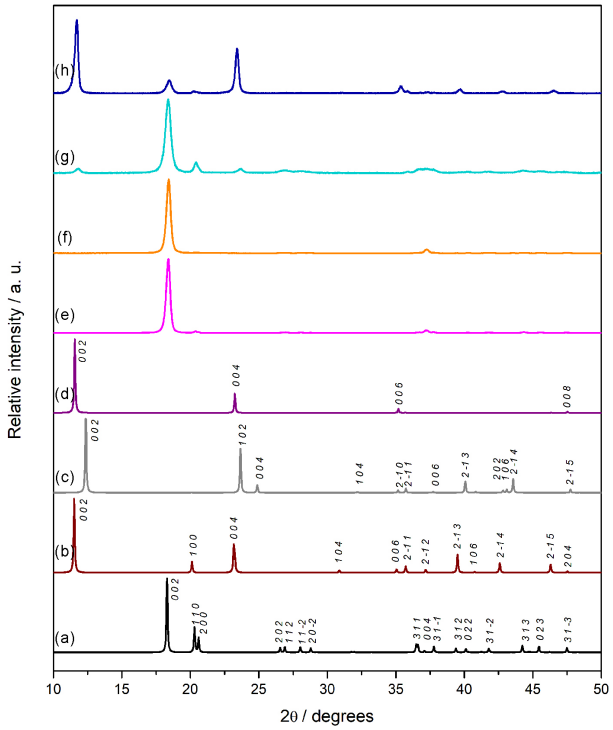

Figure 4. PXRD patterns available in the literature for the materials (a) gibbsite (ICSD 36233), (b) dritsite,[33] (c) anhydrous dritsite (ICSD 83509) and (d) hydrated dritsite (ICSD 83512),[9] along with the X-ray diffraction patterns obtained for the synthesized materials (e) LiAl-1, (f) LiAl-2, (g) LiAl-3 and (h) LiAl-4.

In 2019, Zhitova *et al.*[33] reported the existence of a mineral that is part of the lithium-aluminum LDH group called dritsite. Given that there must be natural conditions that lead to the production of this LDH, it was decided to test the effect of exposing gibbsite to an excess of LiCl in aqueous solution. The material obtained was named LiAl-3 and was synthesized from Gib-3.

The X-ray diffraction patterns obtained for LiAl-3 (Figure 4g) exhibit diffraction peaks at 2θ angles from 17 to 20° and after 35°, which refer to gibbsite used in the synthesis, Gib-3. But less intense diffraction peaks were also observed at 2θ angle values from 11 to 13 and from 22 to 25°, which may refer to the hydrated Li/Al LDH, and were absent in the X-ray diffraction pattern of the Gib-3, suggesting the obtainment of a certain amount of Li/Al LDH in the synthesis. These observations highlight the importance of controlling the concentrations of the reagents in the reaction and indicate that the use of concentrated lithium chloride solution for the synthesis of Li/Al LDH is promising.

Although in this second synthesis attempt, the reaction was performed under LiCl saturated solution, it was observed that the reaction solution was no longer saturated after the fourth day of the reaction, since it was in the beginning because an increase in the water volume from 2.5 to almost 4 mL was observed. This observation was probably associated with the fact that LiCl is a very hygroscopic salt (Li^+ has a large charge to radius ratio), so the ion-dipole interaction between the cations and the polar water molecules is large.[75] The salt must have absorbed moisture from the air, leading to dilution of the reaction solution, suggesting again the importance of good control of reagent concentrations for the success of the reaction. Thus, if the solution had been kept supersaturated until the end of the synthesis, Li/Al LDH might have been obtained.

Based on this, the synthesis of LiAl-4 was conducted based on modifications of the method proposed by Hou and Kirkpatrick.[15] This method involved heating gibbsite in the presence of a nearly saturated LiCl solution for 14 h at 90 °C.

According to Figure 4h, the LiAl-4 X-ray diffraction pattern presents diffraction peaks at 2θ angles between 10 and 15°, around 23° and between 35 and 55°. These diffraction peaks are similar to those observed in the X-ray diffraction pattern of dritsite, generated from the CIF (Crystallographic Information File) obtained from Zhitova *et al.*,[33] and are also similar to the diffraction peaks present in the X-ray diffraction pattern of Li/Al LDH hydrated phase, accessed from the Cambridge Structural Database with reference from O'Hare and co-workers.[9] In addition, the X-ray diffraction pattern for LiAl-4 has a diffraction peak at a 2θ angle around 18°, which can be attributed to residual gibbsite. This may indicate that part of the starting gibbsite did not react with LiCl to form the LDH, or that part of the obtained LDH lost lithium cations and intercalated chloride anions with the procedure of washing the solid with water, for example.

During LiAl-4 synthesis, the reaction mixture was so viscous that magnetic stirring of the system may have been inefficient. This synthesis condition may have hindered the insertion of lithium into the $Al(OH)_3$ unoccupied sites and chloride ions between the layers of a certain portion of gibbsite. Also, it is possible that part of the LDH formed during the synthesis had the lithium ions deintercalated from the layers in the washing step with water, since this LDH has been in some extent reported in the literature

to have this ability of being formed by incorporation of lithium salts in aluminum hydroxides structures, but also this reaction is reversible in some extents and conditions that can get to a point of restoring the gibbsite. This property has already been explored, for example, in the extraction and purification of lithium from aqueous resources and brines.[12,13,73]

TEM and SEM images of LiAl-4 indicated the maintenance Gib-7 of pseudohexagonal platelet like morphology in the synthesized LDH (Figure 5).

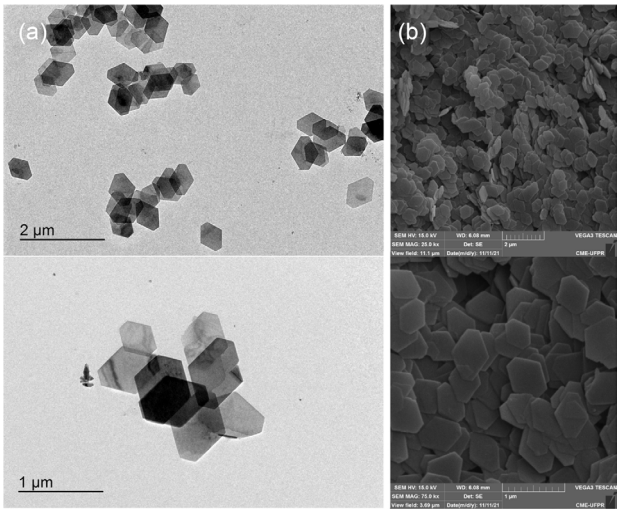

Figure 5. (a) TEM and (b) SEM images of the LiAl-4 material at different magnifications.

The SAED spectra of both solids were also obtained. This characterization showed hexagonal patterns for the LiAl-4 solid, distinct from Gib-7 (Figures S1-S4, Supplementary Information (SI) section). This is in good agreement with the literature, since the Li/Al LDH pattern matches the one obtained for LiAl-4.[18] Also, it was possible to calculate the cell parameters for the LiAl-4 solid, where the parameters a = b = 5.05 Å are very close to the ones reported by O'Hare and co-workers[9] and those attributed to dritsite.[33] That slight difference could have been due to the residual presence of gibbsite in the LiAl-4 solid, which might explain the pattern of small dots with square shape inside the hexagons centered in strong spots.

For comparative purposes, the FTIR measurements for LiAl-4 and Gib-7 were also obtained (Figure 6).

In the Gib-7 FTIR spectrum (Figure 6a), it is possible to observe bands at 3620, 3525, 3475 and 3396 cm^{-1}, all associated to O–H stretching and bending vibration modes. They can be attributed to gibbsite hydroxyl groups. The band at 3620 cm^{-1} is a characteristic band of gibbsite and refers to H-bond stretching between hydroxyl groups in the same plane (the same applies to 3525 cm^{-1}). The other bands of this region are also attributed to H-bonds between hydroxyl groups, but located in different layers.[76,77] The bands at 1384, 1018, 968, 914 cm^{-1} are bending vibrations of Al–O–H bonds, with the band at 914 cm^{-1} corresponding to an Al(OH)Al group with minimal to no hydrogen bonding interactions, while the rest indicate H-bonded OH stretching.[41,76,77] At 804 and 754-756 cm^{-1}, out-of-plane *ν*(OH) bending vibrations can be seen, while the bands at 667, 557 and 516 cm^{-1} refer to Al–O unit bending modes.

Both spectra have similar patterns, but the biggest differences that can suggest the success of the Li intercalation are the disappearance of the band at 3620 cm^{-1} in the LiAl-4 spectrum (Figure 6b), which is characteristic of gibbsite and may indicate a change in the arrangement of the hydroxyl groups with the addition of lithium;[20,74] and the bands in the region of 700-500 cm^{-1}, which are attributed to Al–O unit bending modes, suggesting that the presence of Li in the layer altered that behavior. Also, the lack of bands regarding CO_3^{2-} species (which would otherwise appear at 1370, 1050, 875 and 675 cm^{-1}) may suggest that the intercalation with chloride was successful, with no carbonate contamination.[20]

From the FTIR analyses performed on the prepared LiAl-4 material, it is possible to conclude that the desired

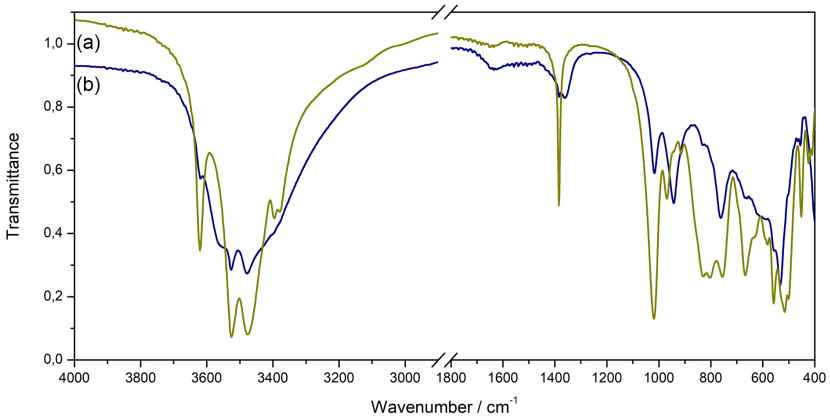

Figure 6. FTIR (KBr pellets) spectra of compounds (a) Gib-7 and (b) LiAl-4.

Li/Al LDH was obtained, although it was mixed with a certain amount of the gibbsite reagent. Future syntheses can be performed with minor changes in the method to favor more efficient stirring of the reaction mixture and possibly reduce the portion of unreacted gibbsite in the final material.

Li/Al LDH was obtained, indicating the synthesis method used may be interesting for preparing other layered anion-exchanging compounds.

Immobilization of an anionic porphyrin on Li/Al LDH

To investigate the property of LiAl-4 to exhibit positive charges on its layered surface, following the example of LDH solids and thus the ability to exchange anions, the immobilization of the free base tetraanionic porphyrin $Na_4[H_2(TSPP)]$ on the LiAl-4 solid was investigated. It was observed that the immobilization of this macrocyclic tetra anionic ligand occurred with a large percentage of immobilization, about 99%, with a loading of 1.3419×10^{-5} mol of porphyrin *per* gram of solid, determined by UV-Vis spectroscopy. The light brown color shown by the LiAl-4-Por solid, in contrast to the white color of LiAl-4 precursor, also suggests that the porphyrin ligand was present in the LiAl-4-Por compound.

The characteristic and intense Soret band of the free base porphyrin $[H_2(TSPP)]$ was observed around 426 nm in the UV-Vis spectra of the solid LiAl-4-Por (Figure 7a), confirming the presence of the porphyrin ligand immobilized in the solid LiAl-4, probably by electrostatic interaction. However, the Soret band is slightly shifted to higher wavelengths compared with the pure porphyrin solid Por (Figure 7c), where the Soret band was observed around 403 nm. The shift behavior observed can be attributed to steric hindrance caused by the support, which can substantially distort the porphyrin molecule, as frequently observed.[78-80]

The LiAl-4-Por solid was also characterized by FTIR, and the spectrum of this material can be compared with those of the Gib-7 and LiAl-4 solids (Figure S5, SI section). The profile of the compared bands suggests that the porphyrin-containing solid still bears similarities in composition to LiAl-4. However, some bands present in the spectrum of Gib-7 had small but noticeable intensity in the spectrum of the LiAl-4-Por material, which suggests that the procedure adopted for the immobilization of porphyrin (which involves dispersion in an aqueous medium) converted part of the Li/Al LDH back into gibbsite, which has been reported in some cases in the literature.[73,74]

The anionic character of the porphyrin used suggests that its immobilization occurred by electrostatic interaction

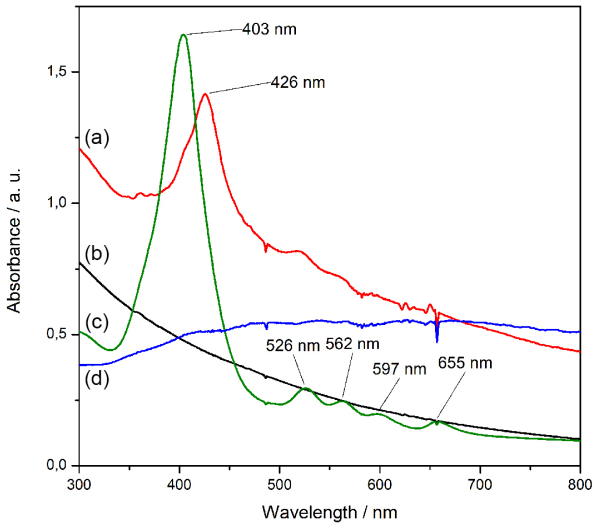

Figure 7. UV-Vis spectra of the following compounds dispersed in mineral oil: (a) LiAl-4-Por, (b) LiAl-4 and (d) Por. UV-Vis spectrum of the solid Por prepared as thin film by the Por dispersion in methanol deposited on a quartz holder and dried at room temperature.

of this ligand with positively charged regions of the LDH layer. This investigation indicates that the gibbsite prepared was a good matrix for the preparation of the LDH. It also suggests the possibility of immobilizing metalloporphyrin on Li/Al LDH for applications in catalysis, with the LDH acting as a solid support.

Conclusions

Gibbsite was prepared with high yield by a simple method proposed by the modification of a synthetic method from the literature, based on mixing an aluminum salt and a base in aqueous media and heating the dispersion obtained. The synthesis proposed was based on the method described by Shen *et al.*,[64] but with a different heating system, consisting of a glass heating flask coupled to a reflux system and heated in an oil bath. Although the best condition we tested in this system involved a longer heating time than used by other authors in a hydrothermal system, this system provided an alternative and more accessible method to synthesize the gibbsite polymorph of $Al(OH)_3$ with high purity, as confirmed by PXRD, SEM and TEM measurements and with an attractive mass yield (76%). The synthesis conditions investigated by this method indicated that longer heating time was associated with higher synthesis yield.

Gibbsite was used to synthesize a Li/Al LDH, which was confirmed by PXRD, with an X-ray diffraction pattern similar to that of the hydrated phase of the hexagonal polytype of the LDH material, which is expected to be obtained when gibbsite was used as precursor. Only the synthesis method proposed by Hou and Kirkpatrick[15] led

to the LDH material, indicating high concentrations of LiCl are required for the LDH synthesis.

Finally, gibbsite and Li/Al LDH were used as supports for the immobilization of an anionic porphyrin, which was immobilized with high percentage of immobilization (99%) and loading of the order of 10^{-5} mol of porphyrin *per* gram of solid.

These studies suggest that Li/Al LDH and also gibbsite alone are interesting supports for the immobilization of anionic catalytic species, demonstrating its potential as a support for porphyrins, since the loadings and percentage of immobilization obtained for the free base porphyrin in this work are numerically close to the ones generally used for the preparation of heterogeneous catalysts based on these species, already reported in the literature with good results in catalysis.[5-8] Moreover, the immobilization experiment by us suggests other species with similar characteristics could be immobilized in these solids for various other applications.

Supplementary Information

Supplementary information about SAED analysis performed for Gib-7 and LiAl-4 is available free of charge at http://jbcs.sbq.org.br as PDF file.

Acknowledgments

We are grateful to Coordenação de Aperfeiçoamento de Pessoal de Nível Superior (CAPES - Finance code 001 and CAPES-PrInt/PROCESSO 88881.311981/2018-01), Conselho Nacional de Desenvolvimento Científico e Tecnológico (CNPq: SN projects 301876/2019-3 and 405217/2018-8; FW Project 300988/2019-2), Fundação Araucária, and Centro de Microscopia da UFPR (CME/UFPR).

Author Contributions

S. Nakagaki and F. Wypych were responsible for the conceptualization, data curation review and editing; S. Nakagaki for project administration, resources, supervision and funding acquisition; G. Bosa, C. G. Silva, B. R. Brito, C. M. Terzi for investigation, data treatment, visualization, validation and writing the original draft.

References

1. Zucca, P.; Neves, C. M. B.; Simões, M. M. Q.; Neves, M. G. P. M. S.; Cocco, G.; Sanjust, E.; *Molecules* **2016**, *21*, 964. [Crossref]
2. Crepaldi, E. L.; Valim, J. B.; *Quim. Nova* **1998**, *21*, 300. [Crossref]
3. Kim, D.; Jung, J.; Ihm, J.; *Nanomaterials* **2018**, *8*, 375. [Crossref]
4. Dutta, P. K.; Puri, M.; *J. Phys. Chem.* **1989**, *93*, 376. [Crossref]
5. Shen, C.; Ma, J.; Zhang, T.; Zhang, S.; Zhang, C.; Cheng, H.; Ge, Y.; Liu, L.; Tong, Z.; Zhang, B.; *Appl. Clay Sci.* **2020**, *187*, 105478. [Crossref]
6. Nakagaki, S.; Halma, M.; Bail, A.; Arízaga, G. G. C.; Wypych, F.; *J. Colloid Interface Sci.* **2005**, *281*, 417. [Crossref]
7. Liu, Y.; An, Z.; Zhao, L.; Liu, H.; He, J.; *Ind. Eng. Chem. Res.* **2013**, *52*, 17821. [Crossref]
8. Nakagaki, S.; Castro, K. A. D. F.; Ucoski, G. M.; Halma, M.; Prévot, V.; Forano, C.; Wypych, F.; *J. Braz. Chem. Soc.* **2014**, *12*, 2329. [Crossref]
9. Besserguenev, A. V.; Fogg, A. M.; Francis, R. J.; Price, S. J.; O'Hare, D.; Isupov, V. P.; Tolochko, B. P.; *Chem. Mater.* **1997**, *9*, 241. [Crossref]
10. Qu, J.; He, X.; Wang, B.; Zhong, L.; Wan, L.; Li, X.; Song, S.; Zhang, Q.; *Appl. Clay Sci.* **2016**, *120*, 24. [Crossref]
11. Roy, S.; Mourad, M. C. D.; Rijneveld-Ockers, M. T.; *Langmuir* **2007**, *23*, 399. [Crossref]
12. Graham, T. R.; Hu, J. Z.; Zhang, X.; Dembowski, M.; Jaegers, N. R.; Wan, C.; Bowden, M.; Lipton, A. S.; Felmy, A. R.; Clark, S. B.; Rosso, K. M.; Pearce, C. I.; *Inorg. Chem.* **2019**, *58*, 12385. [Crossref]
13. Isupov, V. P.; Kotsupalo, N. P.; Nemudry, A. P.; Menzeres, L. T. In *Studies in Surface Science and Catalysis*, vol. 120A, 1st ed.; Dąbrowski, A., ed.; Elsevier: Amsterdam, NL, 1999, p. 621. [Crossref]
14. Fogg, A. M.; Freij, A. J.; Parkinson, G. M.; *Chem. Mater.* **2002**, *14*, 232. [Crossref]
15. Hou, X.; Kirkpatrick, R. J.; *Inorg. Chem.* **2001**, *40*, 6397. [Crossref]
16. Zhang, F.; Hou, W.; *Solid State Sci.* **2018**, *79*, 93. [Crossref]
17. Venkataraman, K.; Pachayappan, L.; *Z. Anorg. Allg. Chem.* **2020**, *646*, 1916. [Crossref]
18. Britto, S.; Kamath, P. V.; *Inorg. Chem.* **2011**, *50*, 5619. [Crossref]
19. Pavel, O. D.; Stamate, A.-E.; Bacalum, E.; Cojocaru, B.; Zăvoianu, R.; Pârvulescu, V. I.; *Catal. Today* **2021**, *366*, 227. [Crossref]
20. Chisem, I. C.; Jones, W.; *J. Mater. Chem.* **1994**, *4*, 1737. [Crossref]
21. French, D.; Schifano, P.; Cortés-Concepción, J.; Hargrove-Leak, S.; *Catal. Commun.* **2010**, *12*, 92. [Crossref]
22. Gupta, S.; Agarwal, D. D.; Banerjee, S.; *Int. J. Polym. Mater. Polym. Biomater.* **2012**, *61*, 985. [Crossref]
23. Wu, Z.; Xie, Z.; Wang, J.; Yu, T.; Wang, Z.; Hao, X.; Abudula, A.; Guan, G.; *ACS Sustainable Chem. Eng.* **2020**, *8*, 12378. [Crossref]
24. Wang, J.; Lei, Z.; Qin, H.; Zhang, L.; Li, F.; *Ind. Eng. Chem. Res.* **2011**, *50*, 7120. [Crossref]

25. Takemoto, M.; Tokudome, Y.; Murata, H.; Okada, K.; Takahashi, M.; Nakahira, A.; *Appl. Clay Sci.* **2021**, *203*, 106006. [Crossref]
26. Kameda, T.; Shinmyou, T.; Yoshioka, T.; *Appl. Surf. Sci.* **2016**, *366*, 523. [Crossref]
27. Zhang, T.; Li, Q.; Xiao, H.; Lu, H.; Zhou, Y.; *Ind. Eng. Chem. Res.* **2012**, *51*, 11490. [Crossref]
28. Zhou, J.; Cheng, Y.; Yu, J.; Liu, G.; *J. Mater. Chem.* **2011**, *21*, 19353. [Crossref]
29. Wei, J.; Gao, Z.; Song, Y.; Yang, W.; Wang, J.; Li, Z.; Mann, T.; Zhang, M.; Liu, L.; *Mater. Chem. Phys.* **2013**, *139*, 395. [Crossref]
30. Yu, M.; Li, H.; Du, N.; Hou, W.; *J. Colloid Interface Sci.* **2019**, *547*, 183. [Crossref]
31. Wang, S.-L.; Lin, C.-H.; Yan, Y.-Y.; Wang, M. K.; *Appl. Clay Sci.* **2013**, *72*, 191. [Crossref]
32. Lin, M.-C.; Chang, F.-T.; Uan, J.-Y.; *J. Mater. Chem.* **2010**, *20*, 6524. [Crossref]
33. Zhitova, E. S.; Pekov, I. V.; Chaikovskiy, I. I.; Chirkova, E. P.; Yapaskurt, V. O.; Bychkova, Y. V.; Belakovskiy, D. I.; Chukanov, N. V.; Zubkova, N. V.; Krivovichev, S. V.; Bocharov, V. N.; *Minerals* **2019**, *9*, 492. [Crossref]
34. Lee, H.; Jeon, Y.; Lee, S. U.; Sohn, D.; *Chem. Lett.* **2013**, *42*, 1463. [Crossref]
35. Nagendran, S.; Periyasamy, G.; Kamath, P. V.; *Z. Anorg. Allg. Chem.* **2015**, *641*, 2396. [Crossref]
36. Chang, Y.-H.; Hsu, H.-Y.; Lin, W.-L.; *Mater. Lett.* **2017**, *194*, 202. [Crossref]
37. Katz, L. E.; Criscenti, L. J.; Chen, C.; Larentzos, J. P.; Liljestrand, H. M.; *J. Colloid Interface Sci.* **2013**, *399*, 68. [Crossref]
38. Wiesner, A. D.; Katz, L. E.; Chen, C.-C.; *J. Colloid Interface Sci.* **2006**, *301*, 329. [Crossref]
39. Girvin, D. C.; Gassman, P. L.; Bolton Jr., H.; *Clays Clay Miner.* **1996**, *44*, 757. [Crossref]
40. Louaer, S.; Wang, Y.; Guo, L.; *ACS Appl. Mater. Interfaces* **2013**, *5*, 9648. [Crossref]
41. Ahmed, I. A.; Al-Radadi, N. S.; Hussein, H. S.; Ragab, A. H.; *J. Chem.* **2019**, *1*, 7685204. [Crossref]
42. Stolyarova, E. A.; Danilevich, V. V.; Klimov, O. V.; Gerasimov, E. Yu.; Ushakov, V. A.; Chetyrin, I. A.; Lushchikova, A. E.; Saiko, A. V.; Kondrashev, D. O.; Kleimenov, A. V.; Noskov, A. S.; *Catal. Today* **2020**, *353*, 88. [Crossref]
43. Chaitree, W.; Jiemsirilers, S.; Mekasuwandumrong, O.; Jongsomjit, B.; Shotipruk, A.; Panpranot, J.; *Catal. Today* **2011**, *164*, 302. [Crossref]
44. Srisawad, N.; Chaitree, W.; Mekasuwandumrong, O.; Shotipruk, A.; Jongsomjit, B.; Panpranot, J.; *React. Kinet., Mech. Catal.* **2012**, *107*, 179. [Crossref]
45. Prabu, S.; Wang, H.-W.; *Int. J. Energy Res.* **2021**, *45*, 9518. [Crossref]
46. Cao, J.; Mei, S.; Jia, H.; Ott, A.; Ballauff, M.; Lu, Y.; *Langmuir* **2015**, *31*, 9483. [Crossref]
47. Wu, G.; Liu, G.; Li, X.; Peng, Z.; Zhou, Q.; Qi, T.; *RSC Adv.* **2019**, *9*, 5628. [Crossref]
48. Asselman, K.; Radhakrishnan, S.; Pellens, N.; Chandran, C. V.; Houlleberghs, M.; Xu, Y.; Martens, J. A.; Sree, S. P.; Kirschhock, C. E. A.; Breynaert, E.; *Chem. Mater.* **2022**, *34*, 7159. [Crossref]
49. Melo, C. C. A.; Melo, B. L. S.; Angélica, R. S.; Paz, S. P. A.; *Appl. Clay Sci.* **2019**, *170*, 125. [Crossref]
50. Shi, Y.; HogenEsch, H.; Regnier, F. E.; Hem, S. L.; *Vaccine* **2001**, *19*, 1747. [Crossref]
51. Reinke, S.; Thakur, A.; Gartlan, C.; Bezbradica, J. S.; Milicic, A.; *Vaccines* **2020**, *8*, 554. [Crossref]
52. Liu, H.; Zhou, C.; An, J.; Song, Y.; Yu, P.; Li, J.; Gu, C.; Hu, D.; Jiang, Y.; Zhang, L.; Huang, C.; Zhang, C.; Yang, Y.; Zhu, Q.; Wang, D.; Liu, Y.; Miao, C.; Cao, X.; Ding, L.; Zhu, Y.; Zhu, H.; Bao, L.; Zhou, L.; Yan, H.; Fan, J.; Xu, J.; Hu, Z.; Xie, Y.; Liu, J.; Liu, G.; *Vaccine* **2021**, *39*, 7001. [Crossref]
53. Palacios, R.; Patiño, E. G.; de Oliveira Piorelli, R.; Conde, M. T. R. P.; Batista, A. P.; Zeng, G.; Xin, Q.; Kallas, E. G.; Flores, J.; Ockenhouse, C. F.; Gast, C.; *Trials* **2020**, *21*, 853. [Crossref]
54. Liang, Z.; Zhu, H.; Wang, X.; Jing, B.; Li, Z.; Xia, X.; Sun, H.; Yang, Y.; Zhang, W.; Shi, L.; Zeng, H.; Sun, B.; *Front. Immunol.* **2020**, *11*, 589833. [Crossref]
55. Centers for Disease Control and Prevention (CDC), *Adjuvants and Vaccines*, https://www.cdc.gov/vaccinesafety/concerns/adjuvants.html, accessed in May 2023.
56. Vrieling, H.; Kooijman, S.; de Ridder, J. W.; Thies-Weesie, D. M. E.; Soema, P. C.; Jiskoot, W.; van Riet, E.; Heck, A. J. R.; Philipse, A. P.; Kersten, G. F. A.; Meiring, H. D.; Pennings, J. L.; Metz, B.; *J. Pharm. Sci.* **2020**, *109*, 750. [Crossref]
57. Zhang, Y.; Zeng, G.; Pan, H.; Li, C.; Hu, Y.; Chu, K.; Han, W.; Chen, Z.; Tang, R.; Yin, W.; Chen, X.; Hu, Y.; Liu, X.; Jiang, C.; Li, J.; Yang, M.; Song, Y.; Wang, X.; Gao, Q.; Zhu, F.; *Lancet Infect. Dis.* **2021**, *21*, 181. [Crossref]
58. Carretero, M. I.; Pozo, M.; *Appl. Clay Sci.* **2010**, *47*, 171. [Crossref]
59. Lombardi, K. C.; Guimarães, J. L.; Mangrich, A. S.; Mattoso, N.; Abbate, M.; Schreiner, W. H.; Wypych, F.; *J. Braz. Chem. Soc.* **2002**, *13*, 270. [Crossref]
60. Gardolinski, J. E.; Martins Filho, H. P.; Wypych, F.; *Quim. Nova* **2003**, *26*, 30. [Crossref]
61. Balena, S. P.; Messerschmidt, I.; Tomazoni, J. C.; Guimarães, E.; Pereira, B. F.; Ponzoni, F. J.; Blum, W. E. H.; Mangrich, A. S.; *J. Braz. Chem. Soc.* **2011**, *22*, 1788. [Crossref]
62. Pozza, A. A. A.; Curi, N.; Guilherme, L. R. G.; Marques, J. J. G. S. M.; Costa, E. T. S.; Zuliani, D. Q.; Motta, P. E. F.; Martins, R. S.; Oliveira, L. C. A.; *Quim. Nova* **2009**, *32*, 99. [Crossref]
63. Britto, S.; Kamath, P. V.; *Inorg. Chem.* **2009**, *48*, 11646. [Crossref]

64. Shen, S.; Chow, P. S.; Chen, F.; Feng, S.; Tan, R. B. H.; *J. Cryst. Growth* **2006**, *292*, 136. [Crossref]
65. Wang, S.; Zhang, X.; Graham, T. R.; Zhang, H.; Pearce, C. I.; Wang, Z.; Clark, S. B.; Jiang, W.; Rosso, K. M.; *CrystEngComm* **2020**, *22*, 2555. [Crossref]
66. Adekola, F.; Fédoroff, M.; Geckeis, H.; Kupcik, T.; Lefèvre, G.; Lützenkirchen, J.; Plaschke, M.; Preocanin, T.; Rabung, T.; Schild, D.; *J. Colloid Interface Sci.* **2011**, *354*, 306. [Crossref]
67. Sweegers, C.; de Coninck, H. C.; Meekes, H.; van Enckevort, W. J. P.; Hiralal, I. D. K.; Rijkeboer, A.; *J. Cryst. Growth* **2001**, *233*, 567. [Crossref]
68. Zhang, X.; Zhang, X.; Graham, T. R.; Pearce, C. I.; Mehdi, B. L.; N'Diaye, A. T.; Kerisit, S.; Browning, N. D.; Clark, S. B.; Rosso, K. M.; *Cryst. Growth Des.* **2017**, *17*, 6801. [Crossref]
69. Freij, S. J.; Parkinson, G. M.; *Hydrometallurgy* **2005**, *78*, 246. [Crossref]
70. Brown, N.; *J. Cryst. Growth* **1972**, *12*, 39. [Crossref]
71. Chesworth, W.; *Clays Clay Miner.* **1972**, *20*, 369. [Crossref]
72. Wierenga, A. M.; Lenstra, T. A. J.; Philipse, A. P.; *Colloids Surf., A* **1998**, *134*, 359. [Crossref]
73. Paranthaman, M. P.; Li, L.; Luo, J.; Hoke, T.; Ucar, H.; Moyer, B. A.; Harrison, S.; *Environ. Sci. Technol.* **2017**, *51*, 13481. [Crossref]
74. Zhong, J.; Lin, S.; Yu, J.; *J. Colloid Interface Sci.* **2020**, *572*, 107. [Crossref]
75. Shriver, D. F.; Atkins, P. W.; Overton, T. L.; Rourke, J. P.; Weller, M. T.; Armstrong, F. A.; *Química Inorgânica*, vol. 1, 4th ed.; Bookman: Porto Alegre, BR, 2008.
76. Kumara, C. K.; Ng, W. J.; Bandara, A.; Weerasooriya, R.; *J. Colloid Interface Sci.* **2010**, *352*, 252. [Crossref]
77. Nguyen, M. K.; Trung, L. G.; Nguyen, H. H.; Tran, N. T.; *J. Taiwan Inst. Chem. Eng.* **2021**, *125*, 332. [Crossref]
78. Westrup, K. C. M.; da Silva, R. M.; Mantovani, K. M.; Bach, L.; Stival, J. F.; Zamora, P. G. P.; Wypych, F.; Machado, G. S.; Nakagaki, S.; *Appl. Catal., A* **2020**, *602*, 117708. [Crossref]
79. Halma, M.; Castro, K. A. D. F.; Taviotgueho, C.; Prevot, V.; Forano, C.; Wypych, F.; Nakagaki, S.; *J. Catal.* **2008**, *257*, 233. [Crossref]
80. Nakagaki, S.; Mantovani, K.; Sippel Machado, G.; Dias de Freitas Castro, K.; Wypych, F.; *Molecules* **2016**, *21*, 291. [Crossref]

Submitted: March 1, 2023
Published online: June 13, 2023